BMC Plant Biology

RESEARCH

Open Access

Genetic dissection of *Meloidogyne incognita* resistance genes based on VIGS functional analysis in *Cucumis metuliferus*

Xiaoxiao Xie[1,2,3,4†], Jian Ling[1†], Junru Lu[1,5], Zhenchuan Mao[1], Jianlong Zhao[1], Shijie Zheng[1], Qihong Yang[1], Yan Li[1], Richard G. F. Visser[2], Yuling Bai[2] and Bingyan Xie[1*]

Abstract

The southern root-knot nematode, *Meloidogyne incognita*, is a highly serious plant parasitic nematode species that causes significant economic losses in various crops, including cucumber (*Cucumis sativus* L.). Currently, there are no commercial cultivars available with resistance to *M. incognita* in cucumber. However, the African horned melon (*Cucumis metuliferus* Naud.), a semi-wild relative of cucumber, has shown high resistance to *M. incognita*. In this study, we constructed an ultrahigh-density genetic linkage bin-map using low-coverage sequences from an F_2 population generated through the cross between *C. metuliferus* inbred lines CM3 and CM27. Finally, we identified a QTL (quantitative trait locus, QTL3.1) with a LOD (logarithm of the odds) score of 3.84, explaining 8.4% of the resistance variation. Subsequently, by combining the results of qPCR (quantitative PCR) and VIGS (virus-induced gene silencing), we identified two genes, *EVM0025394* and *EVM0006042*, that are potentially involved in the resistance to *M. incognita* in CM3. The identification of QTLs and candidate genes in this study serve as a basis for further functional analysis and lay the groundwork for harnessing this resistance trait.

Keywords *Cucumis metuliferus*, *Meloidogyne incognita*, Bin map, QTL, VIGS

Introduction

The southern root-knot nematode (*Meloidogyne incognita* (Kofoid & White) Chitwood), can cause serious damage to plant growth and yield loss around the world. Achieving complete control or eradication of *M. incognita* is unattainable [1]. Among management techniques, nematicides have been effective in controlling nematodes in many crops for decades. Many traditional nematicides with a broad-spectrum, including fumigants (soil sterilant), organophosphates and carbamates (neural toxins), have been banned in recent years due to their potential harm to the environment and humans [1–3]. Thus, the use of *M. incognita*-resistant cultivars would be a more economical and effective approach.

Cucumber (*Cucumis sativus* L., 2n = 14) is an economically important vegetable crop worldwide. It was

†Xiaoxiao Xie and Jian Ling contributed equally to this work.

*Correspondence:
Bingyan Xie
xiebingyan@caas.cn
[1]State Key Laboratory of Vegetable Biobreeding, Institute of Vegetables and Flowers, Chinese Academy of Agricultural Sciences, Beijing 100081, China
[2]Plant Breeding, Wageningen University & Research, Droevendaalsesteeg 1, Wageningen 6708 PB, The Netherlands
[3]Graduate School Experimental Plant Sciences, Wageningen University and Research, Wageningen, The Netherlands
[4]Shanghai Key Laboratory of Protected Horticulture Technology, Shanghai Academy of Agricultural Sciences, Shanghai 201403, China
[5]College of Life Sciences, Beijing Normal University, Beijing 100875, China

cultivated on an area of 2,172,193 ha with a total production of 93,528,796 tons in 2021 (http://faostat.fao.org). However, *M. incognita* can cause severe yield loss of cucumber [4–6]. Among cucumber germplasm accessions, no *M. incognita*-resistant sources were identified and no commercial cucumber cultivars with resistance to the nematode are currently available [7–10].

The African horned melon (*Cucumis metuliferus* Naud., 2n=24) is considered as the wild or semi-wild relative of cucumber and highly resistant to *M. incognita* [4, 10–15]. The resistance in *C. metuliferus* was shown to be associated with hindrance of larval development, with most second-stage juveniles (J2s) delaying development to later stage juveniles and stimulating toward maleness, resulting in few nematodes developing to the adult female stage [4, 16, 17]. Therefore, compared with cucumber or melon, the susceptibility in *C. metuliferus* to root knot nematodes is significantly reduced but not completely absent [4, 10]. However, the efforts to transfer the resistance to cultivars by creating viable interspecific hybrids between cucumber and *C. metuliferus* have encountered serious reproductive barriers, resulting in failure so far [4, 8, 9, 15]. Specifically, no fruit development was observed when *C. metuliferus* was used as the female parent. In crosses where cucumber was used as the female parent, only seedless fruits or fruits with nonviable seed development were observed [8].

In recent years, many researches have been conducted in transcriptomic studies on the incompatible interaction between *C. metuliferus* and *M. incognita* [17–19]. Transcriptomic analysis revealed that multiple signaling pathways, such as salicylic acid (SA), jasmonic acid (JA) and Ca^{2+} signaling, play a positive role in the resistance [19]. In addition, cytoskeleton-related genes may also be involved in resistance [18]. Furthermore, the genes related to phenylpropanoid biosynthesis, plant hormone signal transduction, and plant-pathogen interaction were involved in the resistance in *C. metuliferus* [17]. However, the *M. incognita*-resistant genes in *C. metuliferus* have not been identified yet. In order to harness the resistance, it is important to explore its resistance genes and investigate the underlying mechanisms of resistance to *M. incognita* in *C. metuliferus*.

In this study, we report on QTL mapping to explore the *M. incognita*-resistance in *C. metuliferus* using an F_2 population. The function of candidate genes in QTL regions were identified using qPCR and VIGS. Our results provide valuable information for mining *M. incognita*-resistance in *C. metuliferus*. Furthermore, these candidate genes possess a potential application in cucumber breeding programs for conferring resistance to the nematode.

Results

Phenotypic identification and genetic analysis

The gall numbers and Gall Index (GI) were used to measure susceptibility/resistance of CM3 and CM27 to *M. incognita* (Fig. 1A-C). 40 days after inoculation, the average gall numbers and GI on CM3 were ~29 and 1.2, respectively. The number of galls and GI on CM27 roots (~110 and 3.7) were significantly higher than that on CM3 roots ($P=0.0171<0.05$). The results demonstrated that CM3 is moderately resistant, rather than completely resistant to *M. incognita.* Further, the gall numbers and GI of CM3 and F_1 did not differ significantly ($P=0.8110>0.05$) (Fig. 1B and C). The results revealed that the F_1 population was resistant to *M. incognita*, indicating a dominant resistance. In the two F_2 populations, the histogram of GI indicates the resistance is quantitative (Supplementary Figure S3). Since the CM3 is not completely resistant with a GI between 1 and 2, we divided the F_2 population lines into two groups, resistant (GI=0,1,2) and susceptible (GI=3,4,5). The ratio of the two groups was in accordance with the expected ratio of 3:1 (resistant : susceptible) for a dominant locus (Supplementary Table S2).

Sequencing and SNP identification

We resequenced both parents with 10x depth and 200 F_2 individual plants with 5x depth on an Illumina HiSeq platform and produced clean data for mining SNPs and developing bin markers. In total, 10,071,087 and 13,630,504 clean reads were generated for the CM3 and CM27, respectively. Meanwhile, 7,983,138 clean reads were generated for the 200 F_2-1 population individuals, with more than 85% of the bases higher than Q30 (Supplementary Table S3). By aligning clean reads with the reference genome sequence of *C. metuliferus* (CM27), we obtained 224,978 SNPs in CM3, 12,730 SNPs in CM27, 102,368 SNPs between the parents (Supplementary Table S4). Finally, we obtained 3,126 bin markers with a sliding window of 15 SNPs (Supplementary Table S5).

Construction of a sequence-based *C. Metuliferus* genetic map

3,126 bin markers were filtered prior to linkage analysis. Then, the remaining 3,028 bin markers were used to construct a genetic linkage map. We constructed an ultra-dense genetic map consisting of 12 linkage groups (LG) with 3,028 bin markers, which covered 1,713.07 cM, with an average distance of 0.57 cM between adjacent bin markers (Table 1; Fig. 2A, Supplementary Table S6). The chromosome-level reference genome of *C. metuliferus* was used to evaluate the quality of the genetic map [11]. In a comparison with *C. metuliferus* chromosomes, Spearman's rank-order correlation coefficients for 12 linkage groups ranged from 0.9373 to 0.9984

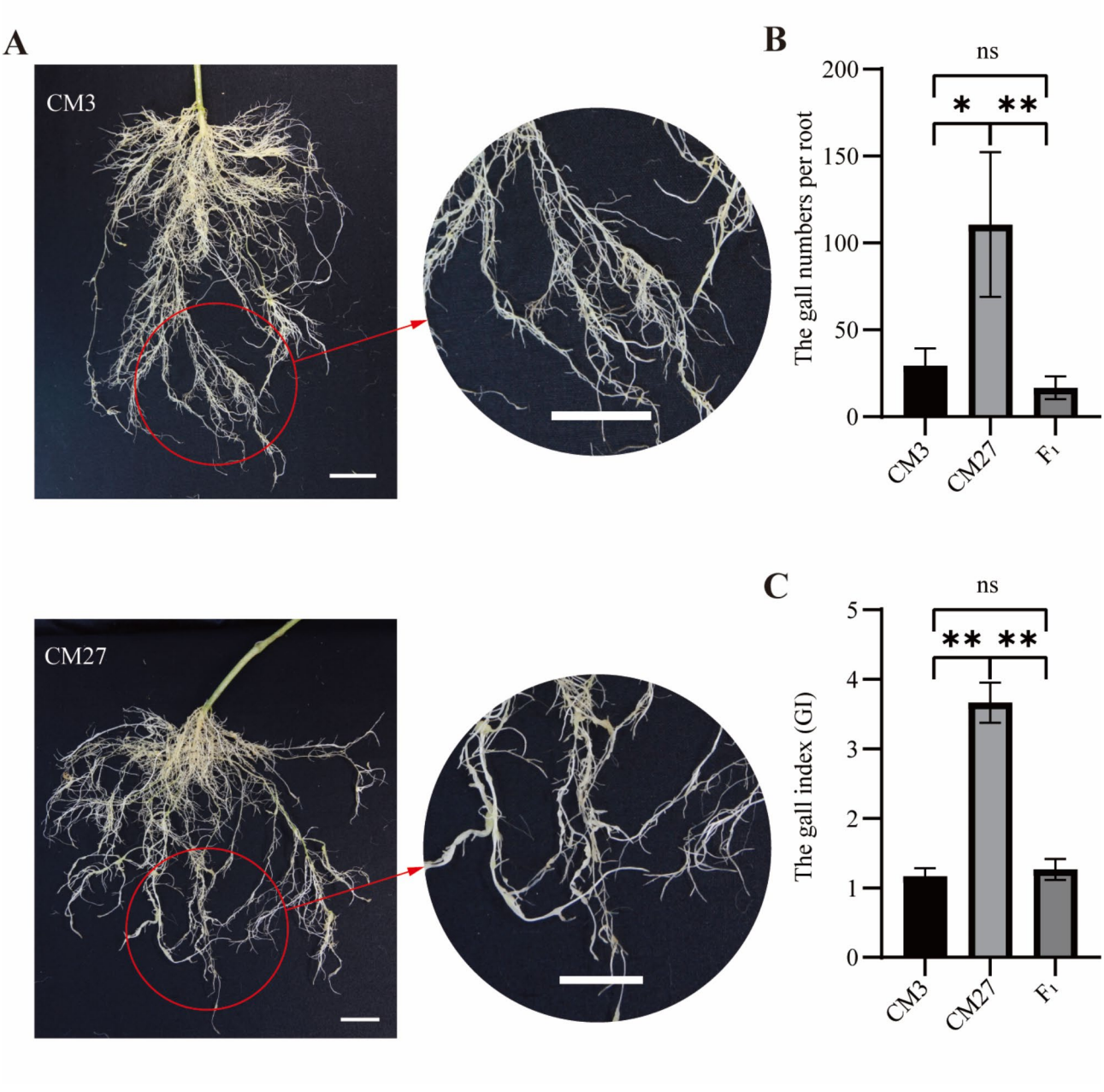

Fig. 1 Phenotyping of *Meloidogyne incognita* resistance in CM3, CM27 and F_1 population. **A** Roots of CM3 and CM27 at 40 days post-inoculation (dpi). Bar = 2 cm. **B** and **C** Average gall numbers (**B**) and Gall Index (**C**) of CM3, CM27 and F_1 at 40 dpi. Data are presented as means ± standard deviation (SD). $*P<0.05$; $**P<0.01$; ns, not significant (one-way ANOVA following Dunnett's post hoc test)

(Fig. 2B, Supplementary Figure S2). These results imply that a good syntenic relationship exists between the two genomes.

QTL analysis for *M. incognita* resistance in the F_2 population

To identify the candidate genomic region for *M. incognita* resistance in *C. metuliferus*, the IM model in MapQTL 6.0 software was used to detect QTLs. We identified a 37Kb region on chromosome 03 (chr 03) with two bin markers (Block7973 and Block7979) that satisfied the LOD threshold of 3.6 (Fig. 3). The LOD peak value was 3.84, with the phenotypic variation of 8.4%. The QTL was named QTL3.1. The physical interval of the QTL locus was from 25,323,564 bp to 25,360,528 bp on chr03. A total of four candidate genes were annotated in the QTL3.1 region based on the *C. metuliferus* reference genome [11] (Fig. 3).

The first candidate gene, *EVM0025394* at position 25,324,104−25,328,367, encodes Lysine

Table 1 Construction of *Cucumis metuliferus* genetic map

LG ID	Total Bin Marker	Total Distance(cM)	Average Distance(cM)	Max Gap(cM)	Gaps < 5 cM(%)
LG1	149	112.64	0.76	10.48	96.62
LG2	271	168.79	0.62	6.84	99.63
LG3	274	190.71	0.7	9.98	98.53
LG4	116	78.3	0.67	10.67	96.52
LG5	465	160.56	0.35	9.51	99.35
LG6	228	173.83	0.76	8.79	99.12
LG7	207	122.08	0.59	6.94	98.54
LG8	299	126.39	0.42	12.3	99.33
LG9	224	107.04	0.48	14.61	98.21
LG10	181	106.26	0.59	18.91	98.89
LG11	272	181.21	0.67	6.54	99.63
LG12	342	185.28	0.54	7.00	99.41
Total	3028	1713.09	0.57	18.91	98.65

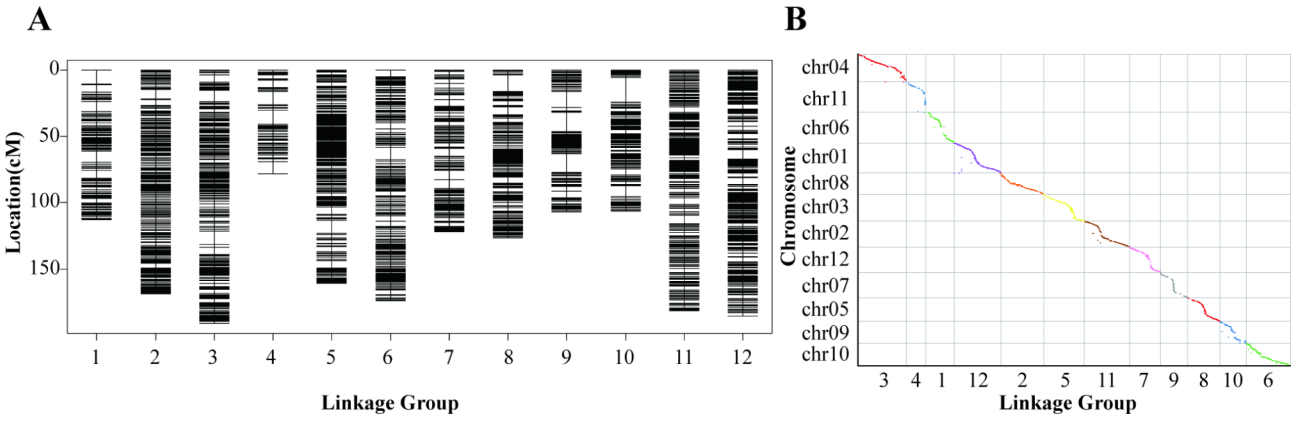

Fig. 2 Genetic map construction and syntenic relationship analysis. **A** The genetic map for the F_2-1 population derived from a cross between CM3 and CM27. Bin markers are located according to genetic distance (cM). **B** Comparison of the syntenic relationships between the linkage groups and chromosomes of *C. metuliferus* using R software. The dots indicate the bin markers

histidine transporter 1. An InterPro analysis indicated that *EVM0006042* (25,335,818−25,338,965) contains a 295-amino acid von Willebrand factor type A domain. *EVM0018474* and *EVM0028872*, located from 25,350,241 to 25,355,854, 25,356,688 to 25,361,129, are predicted to encode COP9 signalosome complex subunit 3 and actin-related protein 2/3 complex subunit 5 A, respectively.

To further screen possible candidate genes underlying the detected QTLs, the CDS sequences of the four candidate genes were cloned and sequenced. We then aligned the CDS sequences of candidate genes between CM3 and CM27. Three nucleotide changes (294th A/T, 1146th G/C and 609th A/G were found at the 294th, 1146th and 609th positions of the CDS respectively in *EVM0028872*, *EVM0018474* and *EVM0025394*), which did not change their amino acid sequences (Supplementary Figure S4). There is no sequence difference in *EVM0006042* between CM3 and CM27.

qPCR analysis

A qPCR analysis was used to assess the expression of these four genes potentially associated with *M. incognita* resistance (Fig. 4). In total, the expression patterns of these candidate genes were analyzed three times in CM3 and CM27 before and after inoculation with *M. incognita*. The expression levels of *EVM0028872* and *EVM0018474* did not change following inoculation in the two materials (Fig. 4E-H). In contrast, *EVM0006042* expression was reduced at 3- and 7-dpi, considerably upregulated in CM3 at 14 dpi (Fig. 4C). However, the opposite expression pattern was found in CM27 at 14 dpi (Fig. 4D). In addition, the expression of *EVM0025394* in CM3 was significantly upregulated from 3 dpi to 14dpi in replicates 1 and 3, and upregulated between 7dpi and 14dpi in replicate 2 (Fig. 4A). Conversely, the *EVM0025394* gene was downregulated in CM27 after inoculation (Fig. 4B). These results indicated that *EVM0006042* and *EVM0025394* are likely the genes responsible for *M. incognita* resistance in CM3.

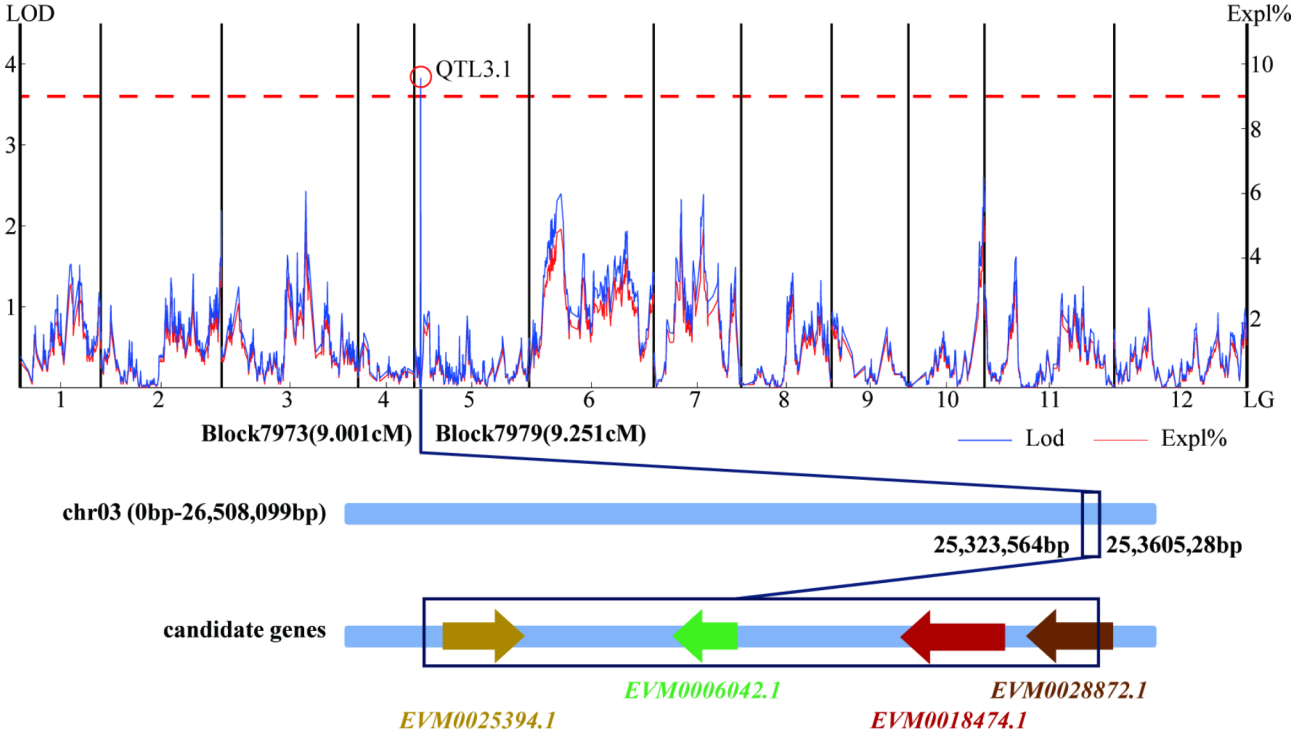

Fig. 3 Mapping of *Meloidogyne incognita* resistance candidate genes on chromosome 03 (corresponding to LG5 in Fig. 2B). QTL mapping of *M. incognita* resistance in the F_2 population. The blue line represents the LOD score and the red line represents the phenotypic variation. The candidate genes in the QTL region are depicted below the mapping interval

Functional verification analysis via VIGs

To further investigate the function of the four candidate genes, the expression of *EVM0025394*, *EVM0006042*, *EVM0018474*, and *EVM0028872* were silenced in CM3 through VIGS (Fig. 5A). The efficiency of the four target genes silencing was established by qPCR. Compared with pV190 control plants, the expression of *EVM0025394*, *EVM0006042*, *EVM0018474*, and *EVM0028872* decreased by approximately 30–80% in the silenced plants (Fig. 5B–D). The number of *M. incognita*-induced galls and root fresh weight were recorded at 40 dpi (Supplementary Figure S5). Then, the number of galls per gram of roots were calculated (Fig. 5E–G). Overall, the number of galls per gram on *EVM0025394*-silenced plants in the three trials were significantly increased compared with the control ($P<0.01$). Similarly, the roots of the *EVM0006042*-silenced plants contained significantly more galls compared with the control ($P<0.05$). However, the number of galls per gram in *EVM0018474*- and *EVM0028872*-silenced lines showed no significant difference compared with that on pV190 plants. Therefore, inhibiting the expression of *EVM0025394* and *EVM0006042* could increase susceptibility to *M. incognita* in CM3.

Discussion

M. incognita has a detrimental impact on the growth and development of cucumber, leading to a decrease in yield [4–6, 20]. Several studies have demonstrated that *C. metuliferus*, an important wild or semi-wild relative of cucumber, exhibits high resistance to *M. incognita* [4, 10–15]. In *C. metuliferus*, it has been observed that only a small number of second-stage juveniles (J2) progress into later stage juveniles (J3/J4) between 10 dpi and 15 dpi [16]. This suggests that hindering larval development is one potential resistance mechanism [4, 16]. Although several transcriptome-based studies have explored the resistant mechanisms, the identification of resistance genes has not yet been undertaken. Consequently, the resistance genes associated with *M. incognita* resistance in *C. metuliferus* remain unreported [17].

In this investigation, we report that *M. incognita* resistance in *C. metuliferus* CM3 may be controlled by a major dominant locus. Moreover, we successfully identified a QTL (QTL3.1) that contains four candidate genes on chr 03. Further qPCR assays on parents determined that the expression levels of *EVM0025394* and *EVM0006042* were upregulated in the roots of the resistant parental CM3 after inoculation, suggesting that these two genes are likely responsible for the resistance to *M. incognita*. To validate this hypothesis, we performed VIGS silencing of the four candidate genes, which resulted in

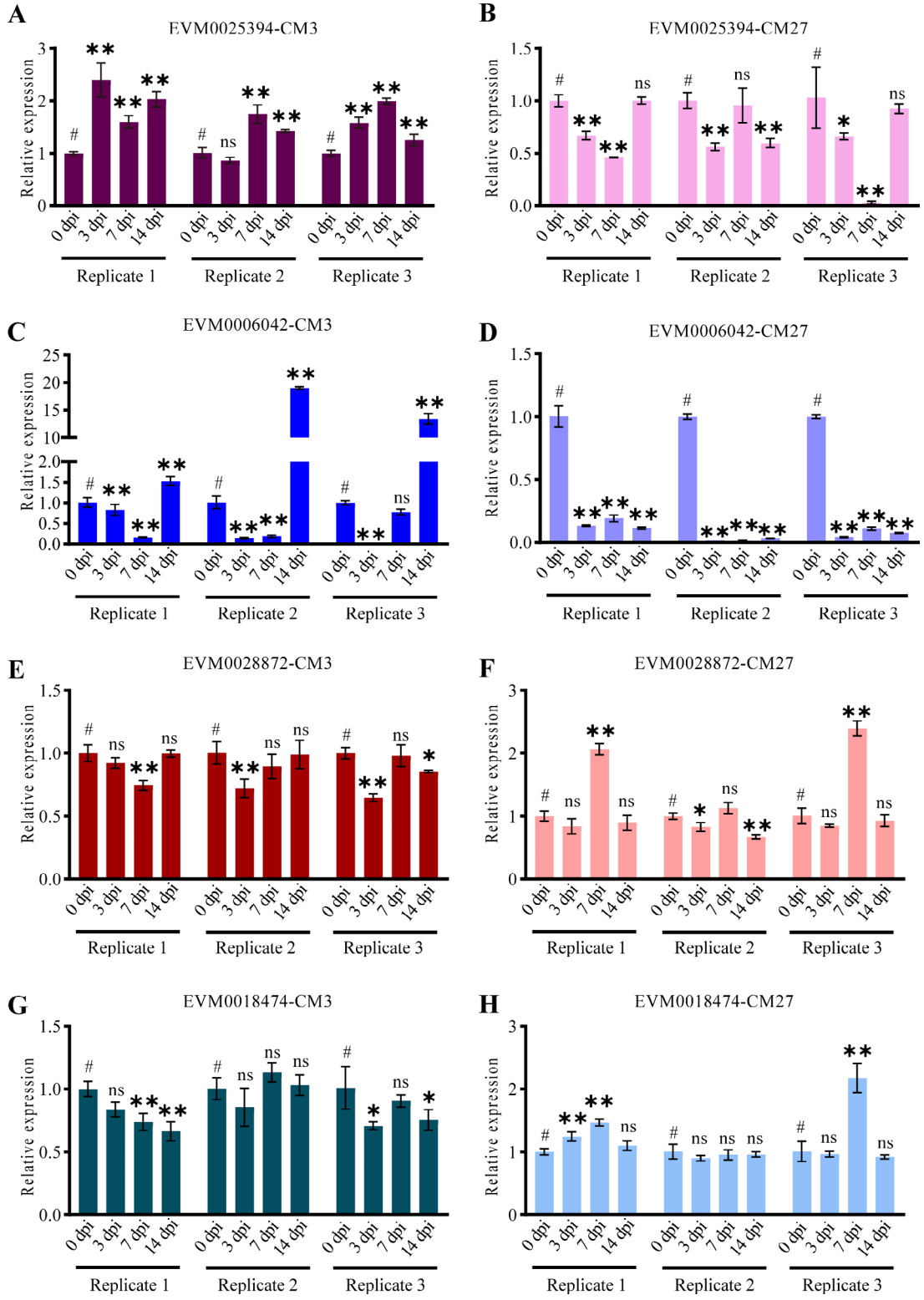

Fig. 4 Analysis of candidate gene expression levels in roots of CM3 and CM27 before and after inoculation with *Meloidogyne incognita*. **A-H** The expression levels of *EVM0025394*(**A**-**B**), *EVM0006042*(**C**-**D**), *EVM0028872*(**E**-**F**), and *EVM0018474*(**G**-**H**) in CM3 and CM27. Relative gene expression was calculated according to the $2^{-\Delta\Delta Ct}$ method. The relative gene expression levels were initially normalized to the levels of the beta-actin gene of *Cucumis metuliferus*, followed by further normalization to the samples at 0 dpi. Data are presented as means ± SD. Asterisks indicate statistically significant differences compared with the control (#) (one-way ANOVA following Dunnett's post hoc test significance, $*P < 0.05$; $**P < 0.01$; ns, not significant)

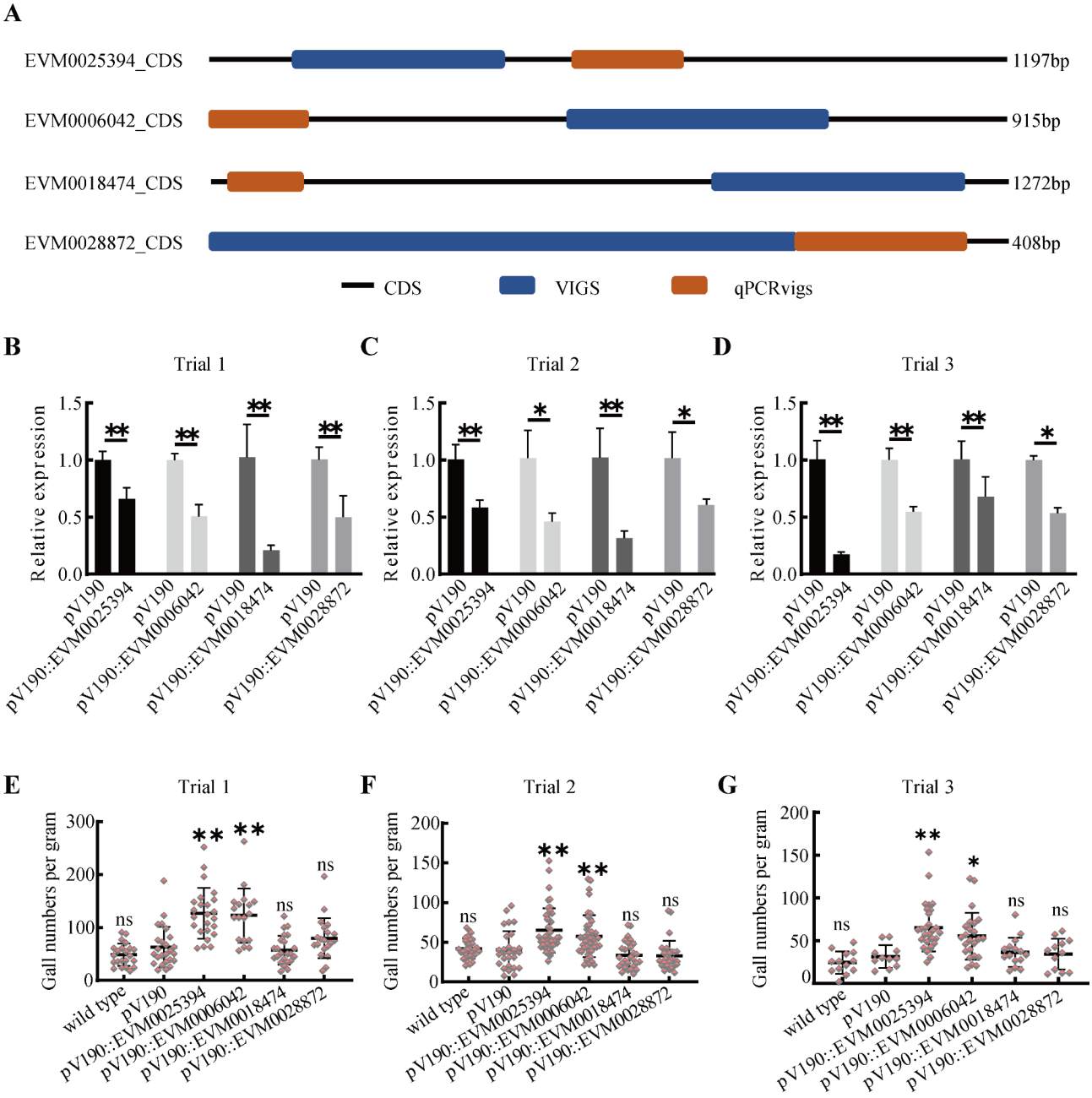

Fig. 5 Silencing of the four candidate genes in CM3. **A** Schematic overview of virus-induced gene silencing of the four candidate genes. **B-D** Relative expression levels of *EVM0025394*, *EVM0006042*, *EVM0018474*, and *EVM0028872* in silenced and control (pV190) plants. Relative gene expression was calculated according to the $2^{-\Delta\Delta Ct}$ method. Gene expressions were normalized to the beta-actin gene of *Cucumis metuliferus*, and subsequently normalized to pV190 plants. Data are presented as means ± SD ($n = 3/4$). *, $P < 0.05$; **, $P < 0.01$ (Student's *t*-test). **E–G** Number of galls per gram of virus-induced gene-silenced plants 40 days post-inoculation. Data are presented as means ± SD. *, $P < 0.05$; **, $P < 0.01$; ns, not significant (one-way ANOVA followed by Dunnett's multiple comparisons test)

increased susceptibility of the roots in *EVM0025394*- and *EVM0006042*-silenced plants to nematodes compared to roots transformed with an empty vector. The VIGS analysis further supported the involvement of these two candidate genes in conferring *M. incognita* resistance at this specific locus.

Among the detected *M. incognita*-resistance candidate genes, *EVM0025394* encodes a Lysine histidine transporter 1 (*LHT1*), which is involved in growth and development in plants and plant pathogens [21]. In Arabidopsis, *AtLHT1* is involved in leaf mesophyll import as well as root uptake of acidic and neutral amino acids (AAs), both at naturally occurring concentrations and

from agricultural soil [22, 23]. Up to now, the role of *AtLHT1* during pathogen infection has been identified in several studies. The expression of *AtLHT1* was induced when the host was infected with various pathogens. However, the hypothesis that *AtLHT1* regulates plant resistance mechanisms is divergent [21]. *AtLHT1* was highly expressed in syncytia and roots when the host was infected with biotrophic nematode *Heterodera schachtii* [24]. Additionally, one of the important substrates of *AtLHT1*, Glutamine (Gln), was observed that its level increased in syncytia when compared to uninfected roots [25]. Based on the above evidences, *AtLHT1* is associated with nematode infection in host. However, *lht1-1* mutants did not exhibit increased resistance to *H. schachtii* [24]. Combining expression and functional verification results, the mechanism of *AtLHT1* regulating nematode resistance is uncertain.

Our findings demonstrate that the expression of *LHT1* is upregulated in CM3 after inoculation and the resistance of CM3 is compromised when the expression is partially suppressed. Our results indicate that *LHT1* may act as a positive regulator in defense against *M. incognita*. A notable example of amino acid transporters acting as nematode resistance genes is *Glyma.18G022400*, a gene located at the *Rhg1* locus that encodes the Rhg1-GmAAT in soybean. The amino acid transporter is one of three genes which are responsible for the resistance to soybean cyst nematode in soybean [26]. This result partially supports our findings.

Another important candidate gene, *EVM0006042*, encodes a protein of unknown function that contains a 295-amino acid von Willebrand factor type A domain. Limited functional studies on this gene family have been conducted in plants. In fact, Von Willebrand factor (VWF) is a large, multimeric glycoprotein that is found in blood plasma, platelet α-granules, and subendothelial connective tissue [27]. The *OVATE* gene, which is homology with human von Willebrand factor genes, is involved in making pear-shaped fruits and was discovered in tomato "Yellow Pear" [28]. It is evident that this function is unrelated to resistance.

In general, the default pathway for *M. incognita* J2s is to enter the root and develop into adult females, which can produce about a thousand eggs through mitotic parthenogenesis [29]. However, certain conditions, such as host stress or nutrient deprivation, can trigger the development of adult males [30, 31]. These males will then abandon their feeding sites and exit the root as a mechanism to maintain an optimal parasitic load for the population's survival [31, 32]. The presence of resistance genes in the host has been identified as one of the masculinizing influences [33]. Similarly, resistance in *C. metuliferus* was associated with hindrance of larval development beyond the second stage, delayed development of larvae to adults and stimulation toward maleness [4, 17–19]. Here, differential expression of *EVM0006042* in CM3 and CM27 suggests its involvement in defense against nematode infestation. Further validation through VIGS supports this hypothesis. Notably, unlike gene *EVM0025394*, the induction of *EVM0006042* expression occurs 14 days after nematode inoculation. At 14 days, about 40% *M. incognita* were developed into females in *C. melo*, while the proportion of females was less than 10% in *C. metuliferus* [34]. Similarly, most of *M. incognita* have developed from J2s into J3/J4 stages in cucumber at 14 dpi. Contrastingly, in *C. metuliferus*, the majority of J2s remained in the J2 stage at the same time point [18]. Therefore, 14 dpi is a pivotal stage in nematode development. Taken together with these previous studies, we speculate that the identified *EVM0006042* is probably not associated with early defense mechanisms, but it might be implicated in nematode development.

In conclusion, our findings would serve as a foundation for deciphering the resistance mechanisms of *C. metuliferus* to *M. incognita*. Current conclusions suggested that the resistance of *C. metuliferus* may be not only controlled by typical resistance genes. However, further research and confirmation of the functions of these two candidate genes are needed, utilizing techniques such as transgenic/genome editing technologies.

Conclusions

In this study, we constructed an F_2 population using a susceptible *C. metuliferus* inbred line (CM27) and a resistant inbred line (CM3). Genetic analysis revealed that the resistance in *C. metuliferus* CM3 inherited dominantly. A QTL on chr 03 was identified. Subsequently, by combining the results of qPCR and VIGS, we identified two genes, *EVM0025394* (encoding Lysine histidine transporter 1) and *EVM0006042* (containing a 295-amino acid von Willebrand factor type A domain), which are potentially involved in the resistance to *M. incognita* in CM3. our findings would serve as a foundation for deciphering the resistance mechanisms of *C. metuliferus* to *M. incognita*. Current conclusions suggest that the resistance of *C. metuliferus* may be not only controlled by typical resistance genes. However, further research and confirmation of the functions of these two candidate genes are needed, utilizing techniques such as transgenic/genome editing technologies.

Materials and methods

Plant materials and nematode resistance screening

C. metuliferus accessions CM3 (accession no. PI 202681) and CM27 (accession no. PI 482460) from the US National Plant Germplasm System (NPGS) were used in this study [13]. After multiple generations of self-crossing, two inbred lines were obtained. An F_1 population

and two F_2 populations (F_2-1 and F_2-2) developed from a cross between CM3 and CM27 were used. The original seed source of CM3, CM27, F_1 population and F_2 populations were provided by Prof. Xingfang Gu of the Department of Cucurbits Genetics and Breeding, Institute of Vegetable and Flowers, Chinese Academy of Agricultural Science. Preparation of nematodes was performed as described in previous studies [35, 36].

The two-leaf stage seedlings were inoculated with approximately 800 *M. incognita* second-stage larvae (J2s). All seedlings were grown with the seedling substrate (peat : vermiculite=1:1 volume ratio) in a greenhouse with day/night temperatures 28/24°C. Approximately 40 days after inoculation, individual F_2 plants, CM3, CM27 and F_1 were scored for their phenotype using a 0–5 galling index (GI) scale. 0=no infection; 1=1–20% of roots galled; 2=21–40% of roots galled; 3=41–60% of roots galled; 4=61–80% of roots galled and 5=81–100% of roots galled (Supplementary Figure S1) [37]. GI was calculated based on the proposition of roots with galls. In addition to GI, the gall numbers of CM3, CM27 and F_1 were also counted.

Sequencing library construction and high-throughput sequencing

Genomic DNA from young leaves of CM3, CM27 and 200 F_2-1 population plants were extracted via the CTAB method [38]. The concentration and quality of DNA were determined by using NanoDrop2000 (Thermo Fisher Scientific). DNA libraries (350 bp) for Illumina sequencing were constructed according to the manufacturer's specifications. Then, sequencing was performed on an Illumina HiSeq NovaSeq platform by a commercial service (Biomarker Technologies, Beijing, China), with 150-bp read lengths.

Genotyping and genetic map construction

Raw reads were filtered and mapped to the *C. metuliferus* genome using the Burrows-Wheeler Aligner software [11, 39]. Duplicates were marked with Samtools, and GATK was used for local realignment and base recalibration [11, 39]. A SNP set was generated by combining GATK and Samtools SNP calling analyses [40]. Polymorphic SNPs between the parents were selected. The SNPs with less than 4x coverage in either parent were removed. The obtained SNPs were scanned by sliding on the genome with 15 SNPs as a window and one SNP as a step. The windows were genotyped as 'aa' or 'bb' when the number of aa-type or bb-type in the window was >12; otherwise, it was genotyped as 'ab'. SNPs without recombination were consolidated into one bin marker. Subsequently, the bin markers exhibiting abnormal patterns, low coverage, or obvious segregation distortions were filtered out. Only markers exceeding 10 Kb in length were retained, and bin markers with abnormal base and segregation distortion ($P<0.01$) were removed.

The selected bin markers were used to construct the genetic linkage map as described previously [41]. Bins were used as markers to construct a high-density genetic map. Marker loci were assigned to linkage groups (LGs) based on their genomic positions. Modified logarithm of odds (MLOD) scores were calculated to validate marker reliability. HighMap strategy was employed for marker ordering and error correction [42]. The collinearity between genetic map and physical map was analyzed via R software and AllMaps [43]. The default parameters were selected when using the above software.

QTL detection

Map-based QTL analysis was performed using interval mapping (IM) implemented by MapQTL6.0 software with IM methods [44]. The permutation test option (1000 permutations) within MapQTL was applied to determine the significance threshold for the LOD. The genome-wide threshold for determining QTL significance in terms of LOD was 3.6 at 95% confidence interval in F_2-1 population.

RNA isolation, cDNA preparation, and quantitative real-time PCR

Leaves or roots were sampled and frozen in liquid nitrogen. Total RNA was isolated using a MiniBEST Plant RNA Extraction kit (Takara, Dalian, China). The extracted RNA was subjected to cDNA synthesis and RT-qPCR analysis employing a PrimeScript RT reagent kit with gDNA Eraser and TB Green Premix Ex Taq II (Takara). RT-qPCR amplifications were performed as previously reported [36]. The RT-qPCR results were analyzed using the $2^{-\Delta\Delta Ct}$ method [45]. The beta-actin gene of *C. metuliferus* was used as an internal control [18]. The experiment was carried out with three biological replicates, each with three or four technical replicates.

Virus-induced gene silencing (VIGS)

The function of the candidate genes was further analyzed using VIGS. The VIGS vector, pV190, has been used for functional verification in several Cucurbitaceae crops successfully [46–50]. Briefly, 300-bp coding sequence fragments of the candidate genes were separately cloned into the pV190 vector. Then, the constructs were introduced into *A. tumefaciens strain* GV3101 as described previously [47, 48]. Two cotyledons of one/two-leaf-stage *C. metuliferus* seedlings were infiltrated with one of the *A. tumefaciens* strains using a syringe. The gene expression level in VIGS plants was detected via qPCR. Plants with significantly downregulated expression were next used to inoculate with nematodes.

Nematode assays in silenced seedlings

The nematode assays were performed as previously described with slight modifications [35]. The silenced seedlings were grown in plastic pots filled with peat and vermiculite (peat : vermiculite = 1:1 volume ratio). Three evenly distributed 5-cm deep holes were created around the roots of the seedlings. Subsequently, 200 J2s were added to each hole using a pipetting gun, resulting in a final inoculation of 600 J2s per seedling. After 40 days, the number of galls and root fresh weight were measured and recorded, the plants transformed with empty pV190 vector acted as control. The VIGS validation of three independent trials were performed, and each trial contained 11– 44 plants.

Primers

Primer design was performed using the online software Primer3Plus (Primer3Plus - Pick Primers). All primers used in this study were listed in Supplementary Table S1.

Statistical analysis

All data were recorded using Microsoft Excel. Statistical analyses were performed using GraphPad Prism and the statistical package IBM SPSS Statistics software.

Abbreviations

QTL	Quantitative trait locus
LOD	Logarithm of the odds
qPCR	Quantitative PCR
VIGS	Virus-induced gene silencing
SA	Salicylic acid
JA	Jasmonic acid
GI	Gall Index
Dpi	Days post-inoculation
LG	Linkage groups
LHT1	Lysine histidine transporter 1
AAs	Acidic and neutral amino acids
VWF	Von Willebrand factor
IM	Interval mapping
MLOD	Modified logarithm of odds

Supplementary Information

The online version contains supplementary material available at https://doi.org/10.1186/s12870-024-05681-6.

Supplementary Material 1: **Supplementary figure S1**. The six rating levels for symptoms evaluation. The scoring scale of 0 to 5 (0 no symptoms and 5 heavily infected) in roots. Scale bars, 2 cm.

Supplementary Material 2: **Supplementary figure S2**. The co-linearity between the genetic map constructed from the F_2 population in this study and a published chromosome-level genomes of *Cucumis metuliferus*.

Supplementary Material 3: **Supplementary figure S3**. The phenotypic distribution of the two F2 populations.

Supplementary Material 4: **Supplementary figure S4**. The gene structure and SNPs in the four candidate genes. They were generated via The Gene Structure Display Server 2.0 (GSDS) (http://gsds.gao-lab.org/). The UTR and CDS are shown in blue and red, respectively. The bases in red and black are in CM3 and CM27 CDS regions.

Supplementary Material 5: **Supplementary figure S5**. The root fresh weight and gall numbers per root of virus-induced gene-silenced plants 40 days post-inoculation. Data are presented as means ± SD. *, $P < 0.05$; **, $P < 0.01$; ns, not significant; #, control (one-way ANOVA followed by Dunnett's multiple comparisons test).

Supplementary Material 6: **Supplementary table S1**. The primers used in this study.

Supplementary Material 7: **Supplementary table S2**. Inheritance of *Meloidogyne incognita* resistance in *Cucumis metuliferus*.

Supplementary Material 8: **Supplementary table S3**. The clean reads were generated for parental lines and 200 F_2-1 population individuals.

Supplementary Material 9: **Supplementary table S4**. The SNPs in parental lines and 200 F_2-1 population individuals.

Supplementary Material 10: **Supplementary table S5**. The bin markers with a sliding window of 15 SNPs.

Supplementary Material 11: **Supplementary table S6**. The bin markers in the genetic map.

Acknowledgements

The authors wish to thank Prof. Qinsheng Gu (Chinese Academy of Agricultural Sciences, China) for providing the cucumber green mottle mosaic virus vector pV190. We also thank Prof. Xingfang Gu (Chinese Academy of Agricultural Sciences, China) for providing C. metuliferus seeds. ChatGPT 3.5 was used for polishing the English text of the introduction and discussion of this manuscript.

Author contributions

B.X., J. Ling. and X.X. designed the experiments. X.X. carried out sampling, DNA extraction and data analysis; J.Lu. and J. Ling. participated in data analysis; Z.M., J.Z., S.Z., Q.Y. and Y.L. helped in the morphological analysis experiments; Y.B., B.X. and R.G.F.V. were responsible for the development and guidance of the project; X.X. wrote the manuscript, and Y.B., B.X. and R.G.F.V. revised the manuscript. All authors read and approved the final manuscript.

Funding

This work was supported by the National Key R & D Program of China (NO. 2023YFD1400400), the National Natural Science Foundation of China (31571996, 32372508), National Agriculture Science and Technology Major Program (NK20220904).

Data availability

Raw Illumina sequencing reads have been deposited in the Genome Sequence Archive (Genomics, Proteomics & Bioinformatics 2021) in National Genomics Data Center (Nucleic Acids Res 2024), China National Center for Bioinformation / Beijing Institute of Genomics, Chinese Academy of Sciences (GSA: CRA019402) that are publicly accessible at https://bigd.big.ac.cn/gsa/browse/CRA019402. All relevant data can be found within the paper and its supporting materials.

Declarations

Ethics approval and consent to participate

Not applicable.

Consent for publication

Not applicable.

Competing interests

The authors declare no competing interests.

Received: 16 February 2024 / Accepted: 8 October 2024
Published online: 15 October 2024

References

1. Shrestha J, Thapa B, Subedi S. Root-knot nematode (Meloidogyne incognita) and its management: a review. J Agric Nat Resour. 2020;3(2):21–31.

2. Desaeger J, Wram C, Zasada I. New reduced-risk agricultural nematicides - rationale and review. J Nematol 2020, 52.
3. Zasada IA, Halbrendt JM, Kokalis-Burelle N, LaMondia J, McKenry MV, Noling JW. Managing nematodes without methyl bromide. Annu Rev Phytopathol. 2010;48:311–28.
4. Fassuliotis G. Resistance of Cucumis spp. to the root-knot nematode, Meloidogyne incognita acrita. J Nematology. 1970;2(2):174.
5. Kayani MZ, Mukhtar T, Growth and yield responses of fifteen cucumber cultivars to root-knot nematode. (Meloidogyne incognita). Acta Scientiarum Polonorum Hortorum Cultus. 2019;18(3):45–52.
6. Kayani MZ, Mukhtar T, Hussain MA. Effects of southern root knot nematode population densities and plant age on growth and yield parameters of cucumber. Crop Prot. 2017;92:207–12.
7. Mukhtar T, Kayani MZ, Hussain MA. Response of selected cucumber cultivars to Meloidogyne incognita. Crop Prot. 2013;44:13–7.
8. Walters SA. TC Wehner Incompatibility in diploid and tetraploid crosses of Cucumis sativus and Cucumis metuliferus. Euphytica 2002;128:371–4.
9. Walters SA, Wehner TC, Barkel KR. Root-knot nematode resistance in cucumber and horned cucumber. HortScience. 1993;28(2):151–4.
10. Wehner TC, Walters SA, Barker KR. Resistance to root-knot nematodes in cucumber and horned cucumber. J Nematology. 1991;23(4S):611.
11. Ling J, Xie X, Gu X, Zhao J, Ping X, Li Y, Yang Y, Mao Z, Xie B. High-quality chromosome-level genomes of Cucumis metuliferus and Cucumis melo provide insight into Cucumis genome evolution. Plant J. 2021;107(1):136–48.
12. Benzioni A, Mendlinger S, Ventura M, Huyskens S. Effect of sowing dates, temperatures on Germination, Flowering, and yield of Cucumis metuliferus. HortScience HortSci. 1991;26(8):1051–3.
13. Weng Y. Genetic diversity among Cucumis metuliferus populations revealed by Cucumber microsatellites. HortScience Horts. 2010;45(2):214–9.
14. Dalmasso A, de Vaulx RD, Pitrat M. Response of some Cucurbita and Cucumis accessions to three Meloidogyne species. Cucurbit Genet Coop 1981:27.
15. Nugent PE, Dukes P. Root-knot nematode resistance in Cucumis species. HortScience. 1997;32(5):880–1.
16. Walters SA, Wehner TC, Daykin ME, Barker KR. Penetration rates of root-knot nematodes into Cucumis sativus and C. Metuliferus roots and subsequent histological changes. Nematropica. 2006;36(2):231–42.
17. Ye DY, Qi YH, Cao SF, Wei BQ, Zhang HS. Histopathology combined with transcriptome analyses reveals the mechanism of resistance to Meloidogyne incognita in Cucumis metuliferus. J Plant Physiol. 2017;212:115–24.
18. Ling J, Mao Z, Zhai M, Zeng F, Yang Y, Xie B. Transcriptome profiling of Cucumis metuliferus infected by Meloidogyne incognita provides new insights into putative defense regulatory network in Cucurbitaceae. Sci Rep. 2017;7(1):3544.
19. Shao H, Fu Y, Zhang P, You C, Li C, Peng H. Transcriptome analysis of resistant and susceptible mulberry responses to Meloidogyne enterolobii infection. BMC Plant Biol. 2021;21(1):338.
20. Fassuliotis G. Plant resistance to root-knot nematodes. Nematology South Region United States Ark Agricultural Exp Stn Fayettev AR USA. 1982;Southern Cooperative Series Bulletin, 276:31–49.
21. Tunnermann L, Colou J, Nasholm T, Gratz R. To have or not to have: expression of amino acid transporters during pathogen infection. Plant Mol Biol. 2022;109(4–5):413–25.
22. Ganeteg U, Ahmad I, Jamtgard S, Aguetoni-Cambui C, Inselsbacher E, Svennerstam H, Schmidt S, Nasholm T. Amino acid transporter mutants of Arabidopsis provides evidence that a non-mycorrhizal plant acquires organic nitrogen from agricultural soil. Plant Cell Environ. 2017;40(3):413–23.
23. Svennerstam H, Jamtgard S, Ahmad I, Huss-Danell K, Nasholm T, Ganeteg U. Transporters in Arabidopsis roots mediating uptake of amino acids at naturally occurring concentrations. New Phytol. 2011;191(2):459–67.
24. Elashry A, Okumoto S, Siddique S, Koch W, Kreil DP, Bohlmann H. The AAP gene family for amino acid permeases contributes to development of the cyst nematode Heterodera schachtii in roots of Arabidopsis. Plant Physiol Biochem. 2013;70:379–86.
25. Hofmann J, El Ashry AEN, Anwar S, Erban A, Kopka J, Grundler F. Metabolic profiling reveals local and systemic responses of host plants to nematode parasitism. Plant J. 2010;62(6):1058–71.
26. Cook DE, Lee TG, Guo X, Melito S, Wang K, Bayless AM, Wang J, Hughes TJ, Willis DK, Clemente TE. Copy number variation of multiple genes at Rhg1 mediates nematode resistance in soybean. *science* 2012;338(6111):1206–1209.
27. Sadler JE. Biochemistry and genetics of Von Willebrand factor. Annu Rev Biochem. 1998;67(1):395–424.
28. Liu J, Van Eck J, Cong B, Tanksley SD. A new class of regulatory genes underlying the cause of pear-shaped tomato fruit. Proc Natl Acad Sci. 2002;99(20):13302–6.
29. Marella HH, Nielsen E, Schachtman DP, Taylor CG. The amino acid Permeases AAP3 and AAP6 are involved in Root-Knot Nematode Parasitism of Arabidopsis. Mol Plant-Microbe Interactions®. 2013;26(1):44–54.
30. Davide R, Triantaphyllou A. Influence of the Environment On Development and Sex differentiation of Root-Knot nematodes. Nematologica. 1967;13(1):111–7.
31. Snyder DW, Opperman CH, Bird DM. A method for generating Meloidogyne incognita males. J Nematology. 2006;38(2):192.
32. Eisenback J. Detailed morphology and anatomy of second-stage juveniles, males, and females of the genus Meloidogyne (root-knot nematodes). Adv Treatise Meloidogyne. 1985;1:47–77.
33. Moura R, Davis E, Luzzi B, Boerma H, Hussey R. Post-infectional development of Meloidogyne incognita on susceptible and resistant soybean genotypes. Nematropica 1993:7–13.
34. Faske T. Penetration, post-penetration development, and reproduction of Meloidogyne incognita on Cucumis melo var. Texanus. J Nematology. 2013;45(1):58.
35. Xie X, Ling J, Mao Z, Li Y, Zhao J, Yang Y, Li Y, Liu M, Gu X, Xie B. Negative regulation of root-knot nematode parasitic behavior by root-derived volatiles of wild relatives of Cucumis metuliferus CM3. Hortic Res. 2022;9:uhac051.
36. Zhao J, Sun Q, Quentin M, Ling J, Abad P, Zhang X, Li Y, Yang Y, Favery B, Mao Z, et al. A Meloidogyne incognita C-type lectin effector targets plant catalases to promote parasitism. New Phytol. 2021;232(5):2124–37.
37. Oka Y, Offenbach R, Pivonia S. Pepper Rootstock Graft compatibility and response to Meloidogyne Javanica and M. Incognita. J Nematology. 2004;36(2):137–41.
38. Wang HJ, Yue WU, Wei GU, Sun XD, Qin ZW. Extraction of DNA from Cucumber by Improved CTAB Method. Heilongjiang Agricultural Sci 2006.
39. Li H, Durbin R. Fast and accurate short read alignment with Burrows-Wheeler transform. Bioinformatics. 2009;25(14):1754–60.
40. Li H, Handsaker B, Wysoker A, Fennell T, Ruan J, Homer N, Marth G, Abecasis G, Durbin R. Genome Project Data Processing S: the sequence Alignment/Map format and SAMtools. Bioinformatics. 2009;25(16):2078–9.
41. Huang X, Feng Q, Qian Q, Zhao Q, Wang L, Wang A, Guan J, Fan D, Weng Q, Huang T, et al. High-throughput genotyping by whole-genome resequencing. Genome Res. 2009;19(6):1068–76.
42. Liu D, Ma C, Hong W, Huang L, Liu M, Liu H, Zeng H, Deng D, Xin H, Song J, et al. Construction and analysis of high-density linkage map using high-throughput sequencing data. PLoS ONE. 2014;9(6):e98855.
43. Tang H, Zhang X, Miao C, Zhang J, Ming R, Schnable JC, Schnable PS, Lyons E, Lu J. ALLMAPS: robust scaffold ordering based on multiple maps. Genome Biol. 2015;16(1):3.
44. van Ooijen JW, Boer MP, Jansen RC, Maliepaard C. MapQTL 6.0, Software for the calculation of QTL positions on genetic maps. Plant Research International, Wageningen, The Netherlands 2009.
45. Livak KJ, Schmittgen T. Analysis of relative gene expression data using real-time quantitative PCR and the 2-DDCt method. Methods. 2001;25(4):402–8.
46. Bi X, Guo H, Li X, Zheng L, An M, Xia Z, Wu Y. A novel strategy for improving watermelon resistance to cucumber green mottle mosaic virus by exogenous boron application. Mol Plant Pathol. 2022;23(9):1361–80.
47. Liu M, Liang Z, Aranda MA, Hong N, Liu L, Kang B, Gu Q. A cucumber green mottle mosaic virus vector for virus-induced gene silencing in cucurbit plants. Plant Methods. 2020;16:9.
48. Xu J, Zhang N, Wang K, Xian Q, Dong J, Qi X, Chen X. Chitinase Chi 2 positively regulates Cucumber Resistance against Fusarium oxysporum f. sp. cucumerinum. Genes (Basel) 2021, 13(1).
49. Zhang Y, Wang Y, Wen W, Shi Z, Gu Q, Ahammed GJ, Cao K, Shah Jahan M, Shu S, Wang J, et al. Hydrogen peroxide mediates spermidine-induced autophagy to alleviate salt stress in cucumber. Autophagy. 2021;17(10):2876–90.
50. Zhu H, He M, Jahan MS, Wu J, Gu Q, Shu S, Sun J, Guo S. CsCDPK6, a CsSAMS1-Interacting protein, affects Polyamine/Ethylene Biosynthesis in Cucumber and enhances salt tolerance by overexpression in Tobacco. Int J Mol Sci 2021, 22(20).

Publisher's note